

Exergoeconomic analysis of the super-long gravity heat pipe geothermal power system: A comparative study with typical single-well geothermal system

Qingshan Ma, Wenbo Huang, Juanwen Chen, Zhibin Li, Fangming Jiang*

*Mailing address, Guangzhou Institute of Energy Conversion, 2 Nengyuan Rd, Tianhe District, Guangzhou, 510640, China.

E-mail address, jiangfm@ms.giec.ac.cn (FM Jiang)

Keywords: Exergoeconomic analysis; Power generation; Single-well geothermal system; Super-long gravity heat pipe.

ABSTRACT

Hot dry rock (HDR) energy is considered as a promising solution of energy shortage and environmental pollution, owing to its ubiquitous distribution and huge reserve. There are two technical routes to exploit the HDR energy: the enhanced geothermal system (EGS) and the single-well system. The novel technical scheme of super-long gravity heat pipe system (SLGHP) in a single-well has aroused widespread interest in the geothermal research and industry community. SLGHP outputs saturated vapor, which can directly drive the turbine to produce electricity, like the thermal power plants. In this study, a thermodynamic and economic model for SLGHP power generation system is established in the outset. A detailed comparison to a typical single-well downhole heat exchanger system (DHE) system is conducted to investigate its performance. Thermodynamic analysis shows that the SLGHP system has higher exergy efficiency compared to the DHE system. The economic analysis indicates that the levelized cost of energy (LCOE) of DHE is much higher than that of the SLGHP. This study unravels the generation performance of the two investigated single-well geothermal systems from the perspective of technology and economy, and the acquired knowledge gives in-depth information of the SLGHP geothermal power generation system.

1. INTRODUCTION

In the upper 10 km of the earth's crust there exists approximately 1.3×10^{27} J geothermal energy, which can be considered as infinite (Lu, 2018). About 98% of the total geothermal resource exists in the form of hot dry rock (HDR) (Geiser, et al., 2016), therefore the efficient exploitation of HDR heat may give the geothermal development a bright future.

The enhanced geothermal system (EGS) and the single-well geothermal system are two main technical routes to exploit the HDR energy. After about 50 years of development, there are still no commercial EGS power plant fully implemented up to now. Numerous problems have been associated with the development of EGS, such as thermal breakthrough, loss of working fluid, scaling of the flow lines, and microseisms resulting from rock fracturing (Li, et al., 2016, Schill, et al., 2015). Large scale artificial reservoir and multiple wells drilling require high initial investment, which combined with grand technical risks may damage the confidence of investors.

As a representative of the traditional single-well geothermal systems, the downhole heat exchanger (DHE) system, is a completely different technology from EGS. The DHE system uses a casing system arranged in a single geothermal well to extract heat from the HDR, and compared to EGS, it has the advantage of avoiding corrosion and scaling of the pipe-lines, as well as loss of the working fluid. The DHE requires only one single well with the consequent reduction in drilling cost. Investigations like numerical simulations on the fluid flow and heat transfer processes and the methods to improve the heat extraction performance on the DHE geothermal system were carried by many researchers (Kohl, et al., 2002, Freeston and Dunstall, 1992). However, the heat extraction rate of DHE is limited by the diminishing temperature difference between the heat reservoir and the working fluid, as the fluid temperature is increased when taking heat from geothermal formation (Huang, et al., 2022). Moreover, in order to drive the fluid flow, DHE system needs to consume pump work (Kohl, et al., 2002, Carotenuto, et al., 2012).

The super-long gravity heat pipe (SLGHP) system was proposed in 2017 (Jiang, et al., 2017), as an alternative technology for HDR heat extraction, which does not necessarily require a fluid-circulation pump (Zohuri, 2016). The working-fluid evaporates and uptakes HDR heat. Since the heat taken by the fluid is stored in the form of latent heat, the heat transfer temperature difference can be maintained, resulting in enhanced heat extraction from the HDR. Compared with DHE, the SLGHP system has lower energy consumption, lower maintenance cost and higher heat extraction rate. However, kilometers-long gravity heat pipe is hard to build because the multiphase flow issues, such as gas-liquid entrainment and stagnant liquid pool effect (Chen, et al., 2021).

Considerable progresses have been made in relation with the development of SLGHP for geothermal exploitation. It was revealed in (Huang, et al., 2018) that the SLGHP system has better heat extraction performance and significantly higher exergy production rate than that of the DHE system. In (Cen, et al., 2021), it was reported that the heat transfer performance of the SLGHP is related with the filling-ratio of working fluid and the multiphase flow status inside. Besides, Key parameters that affect the SLGHP system performance have been figured out in (Huang, et al., 2022), and specially a criterion for SLGHP working fluid fast screening was established in (Chen, et al., 2022). The successful field test (Huang, et al., 2022) corroborated an in-house designed and manufactured super-long heat pipe well performed for HDR heat extraction; The model predictions show good overall agreement with the field test results, verifying the correctness of the developed model.

Electricity generation is one of the main goals of geothermal development. In 2018, the global geothermal power generating capacity reached around 13.3 GW, and was kept growing in the next few years (Lu, 2018, Hutterer, 2020). The geothermal power generation in China is still at an early stage of development with the total installed capacity of 27.78 MW (Zhang, et al., 2019, Hu, et al., 2021).

There were no social barriers for geothermal exploitation in China (Hu, et al.,2021), key technological break-throughs and better economic benefits will release the geothermal energy market potential.

SLGHP outputs saturated vapor, which can be used to directly drive the turbine for electricity production, not like other geothermal power generation systems. Though the power generation capacity of DHE system was studied by some researchers (Noorollahi, et al.,2016), to the best of the authors' knowledge, there is no investigation of SLGHP power generation system is published so far. This paper contributes the thermodynamic and economic modelling of the SLGHP power generation system in the outset. The energy, exergy and levelized cost of energy (*LCOE*) performance analysis are carried out, including the exergy destructions and the overall performances of the

2. SYSTEM DESCRIPTION

Schematic diagrams of the two investigated single-well HDR geothermal power systems - Super-long gravity heat pipe system (left) and coaxial tubular downhole heat exchanger system (right) - are presented in Fig 1.

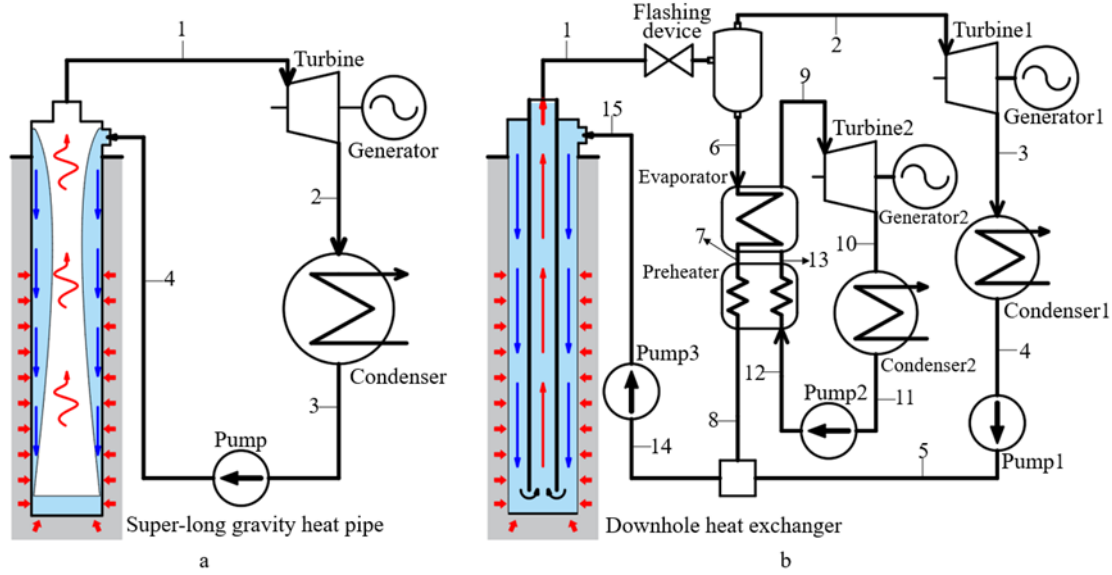


Fig. 1. Schematic diagrams of (a) SLGHP system and (b) DHE system

In the SLGHP geothermal system, the SLGHP is used to extract heat from the underground hot rock, and it produces the saturated vapor continually. The vapor expands through the turbine (state point 1 to 2), which drives the electric generator. Then the vapor leaving the turbine enters the condenser, where through an isobaric process, it releases latent heat and leaves as saturated liquid (state point 2 to 3). Then the liquid is pumped to a pressure equal to that of state point 1, and is then injected into the SLGHP for a new cycle.

In the DHE system, a coaxial tubular downhole heat exchanger is used to extract heat from underground. To improve the heat efficiency (Zhao, et al.,2016), the energy utilization system which combining the flashing system and ORC system is considered in this work. The hot water (state point 1) flows through the flashing device and is separated as saturated vapor (state point 2) and saturated liquid (state point 6). The saturated liquid (state point 6) transfers the heat to the binary organic Rankine cycle (ORC) circuit by the evaporator and preheater. The saturated vapor drives the power system directly and turns into saturated liquid (state point 2-4). And then the saturated liquid is pumped to a pressure equal to that of state point 8, and mixes with the flow at the state point 8. Pump 3 raises the pressure of the mixed flow fluid to P_{15} and a new cycle is initiated.

3. METHODS

The thermodynamic and economic models of the systems are presented in this section, and they are based on the following assumptions:

- No air leakage in all systems;
- Negligible pressure losses of the surface components;
- Ignore the heat loss to the environment;
- Kinetic energy and potential energy are neglected;
- Steady state operation of the system.

The thermodynamic simulation is conducted in the Python environment, which allows the linkage to the fluid database Refprop 9.1.

3.1 Thermodynamic analysis

The energy and mass balances for each component of the system are formulated as (Zhao, et al.,2016):

$$\Delta_{out}^{in} \left(\sum_i m_i \cdot h_i \right) + \Delta_{out}^{in} \left(\sum_j Q_j \right) + \Delta_{out}^{in} \left(\sum_k Q_k \right) = 0 \quad (1)$$

$$\Delta_{out}^{in} \left(\sum_i m_i \right) = 0 \quad (2)$$

The optimal flash temperature of single-flash power system is (Ma, et al.,2022):

$$T_2 = \sqrt{T_1 T_0} \quad (3)$$

The mass flow rate of saturated vapor after the flashing device is:

$$m_2 = \frac{h_1 - h_6}{h_2 - h_6} m_1 \quad (4)$$

The pinch diagram of the evaporator and preheater of the DHE system is shown in Fig 2; with reference to this figure, the mass flow rate of the ORC working fluid can be calculated by the following energy balance equation:

$$Q_{EVA} = m_G (h_6 - h_7) = m_{ORC} (h_9 - h_{13}) \quad (5)$$

ΔT_{ORC} is the pinch point temperature difference, namely:

$$\Delta T_{ORC} = T_7 - T_{13} \quad (6)$$

where, T_{13} is the outlet temperature of the organic working-fluid at the preheater and T_7 is the inlet temperature of the geothermal fluid at the preheater. Then T_8 can be calculated by the preheater energy balance:

$$Q_{PRE} = m_G (h_7 - h_8) = m_{ORC} (h_{13} - h_{12}) \quad (7)$$

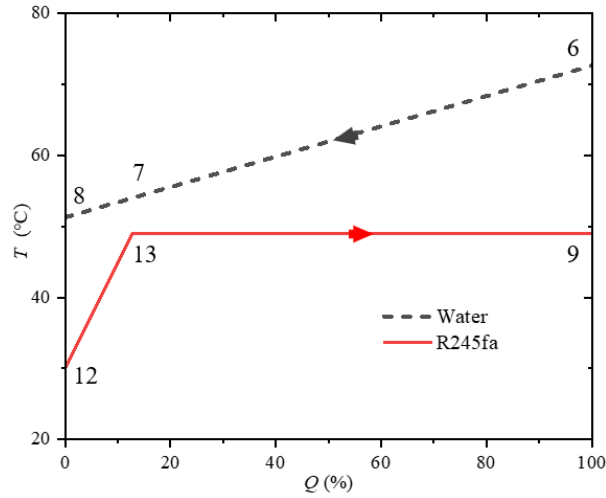


Fig. 2. Pinch diagram of the heat exchange

The net output of the system is calculated by:

$$W_{net} = G_{net} - W_{pump} \quad (8)$$

The energy efficiency of the whole system is defined as the ratio between the net electrical power output and the total thermal power input:

$$\eta_{en} = \frac{W_{net}}{Q_{in}} \quad (9)$$

The exergy flow for each thermodynamic state is calculated by:

$$ex = (h - h_0) - T_0 \cdot (s - s_0) \quad (10)$$

The exergy destruction/loss of each component can be evaluated as (Leveni, et al.,2019):

$$Ex_L = Ex_{in} - Ex_{out} \quad (21)$$

The exergy efficiency of the whole system is defined as the ratio of the exergy of the output power to the input exergy:

$$\eta_{ex} = \frac{W_{net}}{Ex_{in}} \quad (32)$$

The pressure loss caused by the resistance along the DHE is calculated by the Darcy-Weisbach equation (Ouyang and Aziz,2016), as follows:

$$\Delta P = \lambda L \frac{\rho V^2}{2d} \quad (43)$$

$$\left\{ \begin{array}{l} \text{For laminar flow: } \lambda = 64 / \text{Re} \\ \text{For turbulent flow: } \frac{1}{\lambda^{0.5}} = -1.8 \log \left[\left(\frac{\varepsilon/d}{3.7} \right)^{1.11} + \frac{6.9}{\text{Re}} \right] \end{array} \right. \quad (54)$$

The pressure loss in the SLGHP is recovered by requiring no pump power, which means that the SLGHP operates under no forced circulation (Chen, et al.,2022).

3.2 Economic analysis

In this study, the levelized cost of energy (*LCOE*) are selected as the assessment criteria of the economic performance. Firstly, the total system cost (*Ct*) should be calculated, which is the sum of Surface Components Cost (*SCC*) and the subsurface components cost. The first step to evaluate *SCC* can be started with the heat exchanger areas. The logarithmic mean temperature difference method (*LMTD*) is used, which is:

$$LMTD = \frac{\Delta T_A - \Delta T_B}{\ln \frac{\Delta T_A}{\Delta T_B}} \quad (65)$$

ΔT_A is the larger temperature difference between the two streams at the inlet and outlet of the heat exchanger, respectively, while ΔT_B is the smaller one.

LMTD is used to calculate *UA* for the heat exchangers, as follows:

$$UA = \frac{Q}{LMTD} \quad (76)$$

where, *U* is the overall heat transfer coefficient, *A* is the heat exchanger area, and *Q* is the total heat load of the heat exchanger.

The equations determining the values of *SCC* for each component are listed in Table 1.

Table 1 Component cost equations (Wang and Dai,2016, Turton, et al.,2009, Yilmaz,2022):

Component	Cost (CNY)	Assumptions
Preheater	$C_0 (UA/UA_0)^{0.9} a$	$C_0=2.2\text{M};$ $UA_0=650 \text{ kW/K}$
Evaporator	$C_0 (UA/UA_0)^{0.9} a$	$C_0=12.5\text{M};$ $UA_0=4000 \text{ kW/K}$
Turbine	$C_0 (W_{TUR})^{0.75}$	$C_0=31 \text{ k}$
Generator	$C_0 (W_{GEN}/W_{GEN,0})^{0.67}$	$C_0=1.7\text{M}; W_{GEN,0}=5000\text{kW}$

Condenser	$C_0(A)^{0.514}$	$C_0=14k$
Pump	$C_0(W_{PUM})^{0.8}$	$C_0=7.3k$
Flashing device	$C_1m + C_2m^{0.67}$	$C_1=0.8k;$ $C_2=2k$

The heat exchanging equipment of the binary DHE system is based on the shell and tube heat exchanger arrangement. The effect of the maximum pressure in the heat exchanger is taken into account by means of the pressure correction factor proposed in (Astolfi, et al.,2014), that is:

$$a = 10^{(a_1 + a_2 \log(p) + a_3 \log^2(p))} \quad (87)$$

where a_1 , a_2 , a_3 are constants, which are reported in Table 2.

Table 2 Constants of pressure factors for the heat exchangers (Turton, et al.,2009)

Type	Pressure (bar)	a_1	a_2	a_3
Preheater	<6	0	0	0
	6-141	-0.00164	-0.00627	0.0123
Evaporator	<6	0	0	0
	6-141	0.03881	-0.11272	0.08183

The cost of the subsurface components is calculated based on Eqs. (18-21); however, the well drilling cost is affected by many factors, like the geological conditions, well location, drilling technology adopted, well diameter and the number of wells being drilled in the same site and so on. Therefore, an accurate estimate of this cost is difficult, and the value given by Eq. (16) should be considered as a first approximation. The cost of the super-long gravity heat pipe is established based on the data of the experimental site in Tangshan (Huang, et al.,2022). It should be mentioned this is a customized experimental SLGHP and, with further commercialization, its cost may be largely reduced.

The well drilling cost is given as (Huang, et al.,2019):

$$C_{wd} = P_d \times H(H+1000)/2000 \quad (98)$$

in which, H is the drilling depth and P_d is the drilling unit-cost, 106 CNY/m. If the single-well geothermal system is used for power generation on a larger scale, multiple wells need to be drilled in the same site. It will reduce the transportation cost of drilling equipment and increase the process effectiveness due to further staff's familiarity with the geological conditions. It is assumed, in case of multiple wells, they all share the same surface equipment, and the total drilling cost can be estimated on the basis of one single well cost, as follows:

$$C_{wdn} = n \times C_{wd} \times 0.8^{\log_2(n)} \quad (109)$$

where n is the number of wells.

The SLGHP (Huang, et al.,2022) and the DHE (Huang, et al.,2019) costs are given as follows:

$$C_{SLGHP} = P_S \times H \quad (20)$$

$$C_{DHE} = P_D \times H \quad (211)$$

in which, P_S (1000 CNY/m) and P_D (600 CNY/m) are the unit-price of SLGHP and DHE, respectively.

To take into account inflation, the costs of all components can be updated to the present year by using the Chemical Engineering Plant Cost Index (CEPCI) using the following relation:

$$C_{pre} = C_{ref} \frac{CEPCI_{pre}}{CEPCI_{ref}} \quad (22)$$

The $LCOE$ is defined as (Lu, et al.,2018):

$$LEOC = \frac{C_t \cdot CRF + OC}{\tau G_{net}} \quad (23)$$

where τ is the power station operation time per year, OC is the operating cost.

$$OC = C_{WW} + C_{Mt} + C_{Mg} \quad (24)$$

where, C_{WW} is wages for workmen, 80000CNY/year/person; C_{Mt} is maintenance cost, calculated as 2% of SCC ; C_{Mg} is management cost.

$$C_{Mg} = 2.5\% \times (C_{WW} + C_{Mt}) \quad (25)$$

CRF is the investment recovery factor.

$$CRF = \frac{(i+1)^t \cdot i}{(i+1)^t - 1} \quad (26)$$

where i is the interest rate, t is the power station service life (years).

4. RESULTS AND DISCUSSION

In order to perform the thermodynamic and economic analysis of the two proposed systems, the same geothermal conditions are considered. The comparison of heat extraction performance between the SLGHP system and the DHE system was previously investigated (Huang, et al.,2018), and the obtained results in (Huang, et al.,2018) are used as inputs for the calculations of the present study, as reported in Table 3. It is noteworthy that in (Huang, et al.,2018) the mass flow rate of heat pipe working fluid was not explicitly stated, and the values listed in Table 3 are derived based on the heat extraction data.

Table 3 Input parameter values in the simulation(Huang, et al.,2018).

Type	Parameter	Value
SLGHP	T_{S1}	393.15K
	m_{S1}	0.3915kg/s
DHE	T_{D1}	401.07K
	m_{D1}	1.908 kg/s
	ΔT_{EXC}	5K
	T_0	298.15K
General	ΔT_{CON}	5K
	H	4000m
	Turbine efficiency	80%
	Pump efficiency	80%
	Electric generator efficiency	90%
	Interest rate	5%
	Power station service life	20 years
	Number of wells	n
	Number of workmen	$n+1$
	Power station operation time per year	8000 hours

4.1 Thermodynamic analysis

Production temperature T_1 is the most important parameters of a geothermal system, which indicates the thermal production quality. The thermodynamic performance comparison between SLGHP and DHE systems as a function of T_1 is shown in Fig 3. From the figure, the energy efficiency of both systems increases linearly with increasing T_1 ; however, the SLGHP system efficiency increases at a higher rate, which is an indication of enhanced performance as the temperature of the geothermal source increases. For T_1 at 80 °C, the energy efficiency of SLGHP system is 9.78%, which is more than twice that of the DHE system, and only when T_1 reaches 180 °C, the energy efficiency of DHE system attains to this value. High temperature geothermal sources are limited by natural conditions and they are scarce; using SLGHP in a geothermal power system is equivalent to significantly improving the quality of

the geothermal resources. The exergy efficiency of the SLGHP system also increases with the increase of T_1 , and its growth rate gradually slows down because it is getting close to the maximum value.

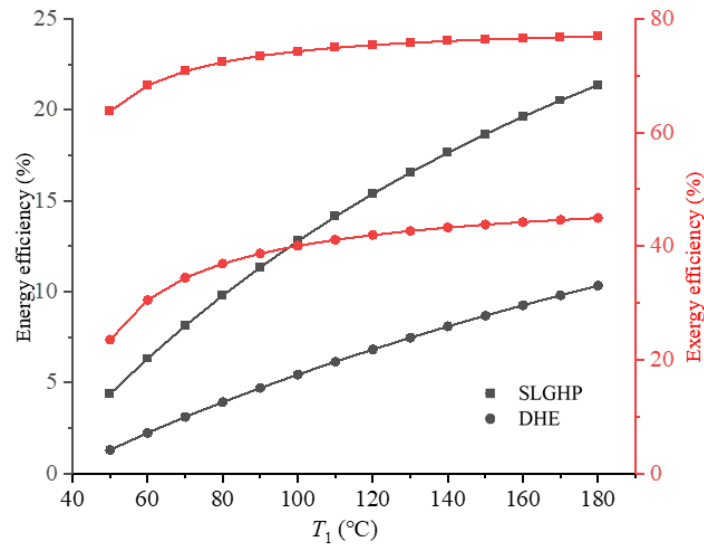


Fig. 3. Energy and exergy efficiency performance comparison between SLGHP and DHE systems as a function of T_1

The exergy losses in each composing component for both systems are calculated, and the relative values and absolute value are plotted in Fig 6. The exergy analysis helps further understand why the SLGHP system is superior to the DHE system in terms of efficiency. In the DHE system, the highest relative exergy destruction occurs in the flashing process with a value of 18.54%, and the heat exchanging process about 5.13%. These two cause 23.67% of exergy loss in total, which does not occur for the SLGHP system. Because the temperature at point 8 cannot be further lowered, the Ex_{out} of the DHE system is much bigger than that of SLGHP (almost 7%). Another obvious difference between these two systems is that the SLGHP has much more inlet exergy than DHE, shows that SLGHP also has great advantages in terms of the performance of heat extraction from the HDR.

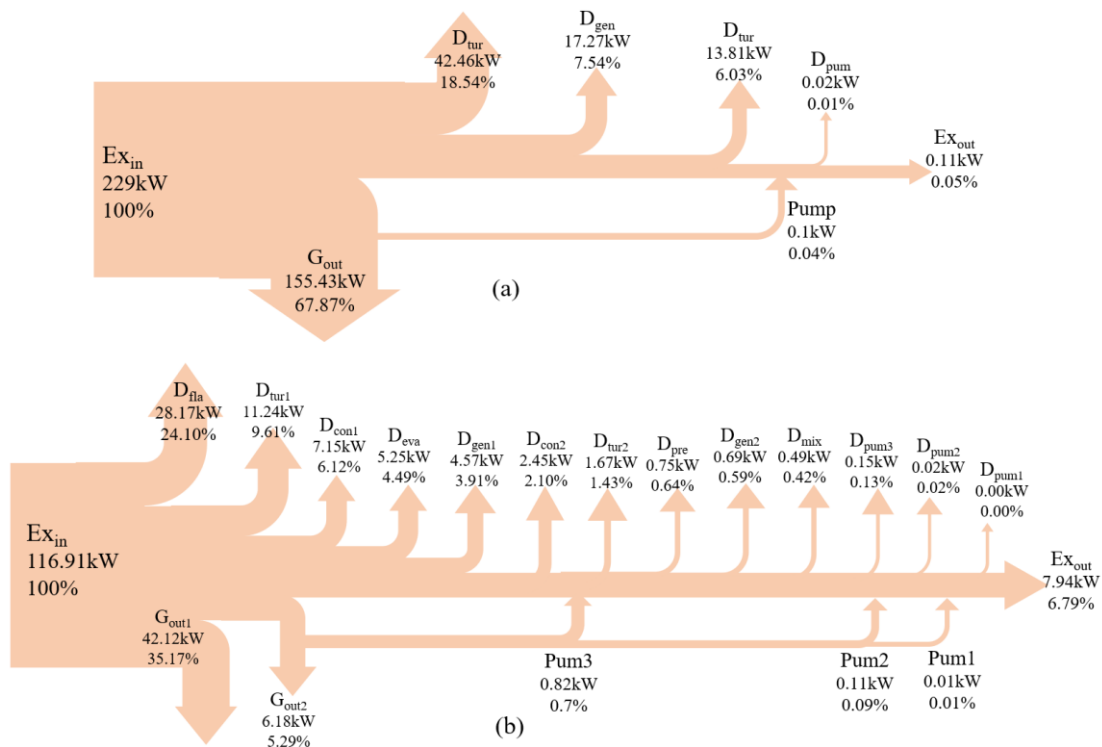


Fig. 4. Exergy flow charts of the: (a) SLGHP system, (b) DHE system

4.2 Economic analysis

The calculated $LCOE$ values as a function of T_1 for the SLGHP and DHE systems are reported in Fig 5. To clearly show the difference between the two systems when the temperature is high, the vertical axis is zoomed in by ten times for T_1 larger than 120 °C in this figure. The $LCOE$ of the SLGHP system is much lower than that of the DHE system for all tested values of T_1 ; with the increase of T_1 , the $LCOE$ of both systems decreases rapidly; for an increase of T_1 from 80 °C to 180 °C, the $LCOE$ of SLGHP system decreases

from 2.44 CNY/kWh to 1.17 CNY/kWh, respectively, and the $LCOE$ of DHE system from 16.47 CNY/kWh to 2.17 CNY/kWh, respectively. Further increase of T_1 narrows the $LCOE$ difference between the SLGHP and DHE systems.

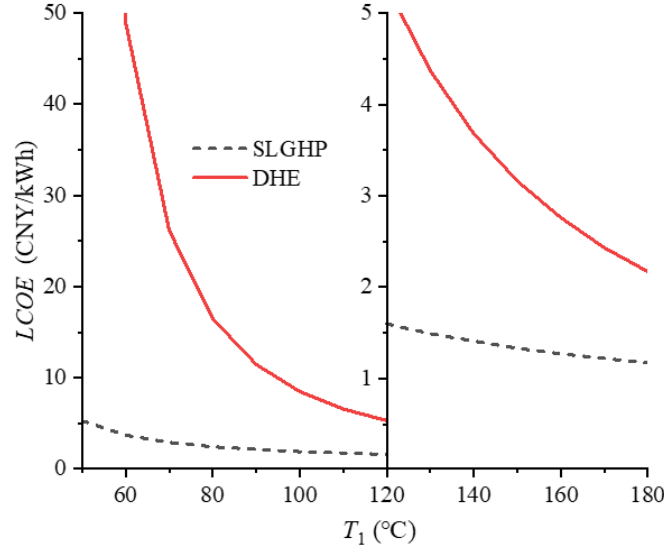


Fig. 5. $LCOE$ as a function of T_1 for SLGHP and DHE system, the vertical axis is zoomed for T_1 larger than 120°C

Following the possibility of using several wells for a single power station, in Fig 6 it is reported the variation of $LCOE$ with the number of wells. By increasing the number of wells, the values of $LCOE$ significantly decrease; the primary explanation for this finding is the reduction at mean drilling cost for the wells, which is realized by reducing the transportation cost of drilling equipment and more effective drilling practice. The sharing of the ground components leads to significant capital savings; in addition, there is the possibility of enhancing the efficiency of the turbines and pumps. The large-scale application shows good market potential.

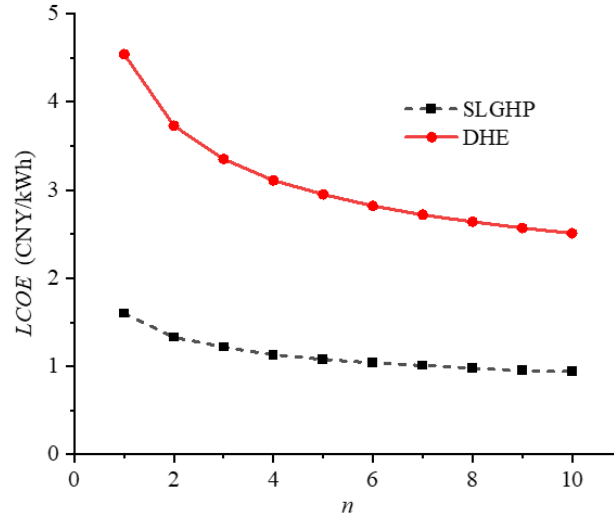


Fig. 6. $LCOE$ as a function of the number of wells for a multi-wells power plant

5. CONCLUSION

To investigate the thermodynamic and economic performance of SLGHP geothermal power system, a comparative study with a typical single-well DHE power generation system is conducted. The main findings in the present study are presented as follow:

- 1) A single-well SLGHP geothermal power generation system can deliver 155.43 kW with the operating conditions of T_1 and m_1 equal to 120 °C and 0.3915 kg/s, respectively. It has much higher energy efficiency than that of the DHE system, for T_1 at 80 °C, the energy efficiency of SLGHP system is 9.78%, and only when T_1 reaches 180 °C, the energy efficiency of DHE system attains to this value.
- 2) The structure of the SLGHP system is relatively simple when compared to that of the DHE system, particularly in what concerns the surface equipment. The extra equipment will not only increase the cost, but also cause more exergy losses. And mainly because the heat exchange can not be completed, the Ex_{out} of the DHE system is found much bigger than that of SLGHP.
- 3) Under the same geothermal conditions, the $LCOE$ of the SLGHP system is 1.60 CNY/kWh, far lower than 4.54 CNY/kWh for the DHE system.

4) By increasing the production temperature T_1 , the economic indicators SLGHP system linearly improve. When T_1 increases from 80°C to 180°C, the $LCOE$ of SLGHP system will decrease from 2.44 CNY/kWh to 1.17 CNY/kWh, and the $LCOE$ of DHE system will decrease from 16.47 CNY/kWh to 2.17 CNY/kWh, respectively.

5) Having a SLGHP geothermal power plant with multiple wells at the same site and sharing the ground equipment may lead to a reduction of the drilling cost per well and to an improvement of other economic indicators. For an increase of the number of wells of the SLGHP geothermal power plant from 1 to 10, $LCOE$ will decrease from 1.60 CNY/kWh to 0.94 CNY/kWh.

The SLGHP system offers a very promising technology for geothermal power generation, and its market competitiveness will be significantly enhanced if drilling costs can be reduced or abandoned oil/gas wells can be used.

REFERENCES

- Lu. A global review of enhanced geothermal system (EGS)[J]. Renewable and Sustainable Energy Reviews, **2018**, 81: 2902-2921.
- Geiser, Marsh, Hilpert. Geothermal: the marginalization of earth's largest and greenest energy source[C]//Proceedings of the 41st workshop on geothermal reservoir engineering, Stanford University, Stanford, SGP-TR-209. 2016.
- Li, Shiozawa, McClure. Thermal breakthrough calculations to optimize design of a multiple-stage Enhanced Geothermal System[J]. Geothermics, **2016**, 64:455-465.
- Schill, Cuenot, Genter, et al. Review of the hydraulic development in the multi-reservoir/multi-well EGS project of Soultz-sous-Forets[C]//Proceedings World Geothermal Congress 2015. Australia: Melbourne, 2015: 19-25.
- Kohl, Brenni, Eugster. System performance of a deep borehole heat exchanger[J]. Geothermics, **2002**, 31(6):687-708.
- Freeston, Dunstall. Rotorua field experiment: downhole heat exchanger performance[J]. Geothermics, **1992**, 21(1-2):305-317.
- Huang, Cen, Chen, et al. Heat extraction from hot dry rock by super-long gravity heat pipe: A field test [J]. Energy, **2022**, 247: 123492.
- Carotenuto, Massarotti, Mauro. A new methodology for numerical simulation of geothermal down-hole heat exchangers[J]. Applied Thermal Engineering, **2012**, 48: 225-236.
- Jiang, Huang, and Cao, et al. Mining hot dry rock geothermal energy by heat pipe: conceptual design and technical Feasibility Study[J]. Advances in New and Renewable Energy, **2017**, vol.5, pp.426-434. (in Chinese).
- Zohuri. Heat pipe design and technology: Modern applications for practical thermal management[M]. Springer, 2016.
- Chen, Cen, Huang, et al. Multiphase flow and heat transfer characteristics of an extra-long gravity-assisted heat pipe: An experimental study[J]. International journal of heat and mass transfer, **2021**, 164: 120564.
- Huang, Cao, Jiang. A Single-Well Geothermal System for Hot Dry Rock Geothermal Energy Exploitation[J]. Energy, **2018**, 162(NOV.1):630.
- Cen, Li, Li, et al. Experimental study of the heat-transfer performance of an extra-long gravity-assisted heat pipe aiming at geothermal heat exploitation[J]. Sustainability, **2021**, 13(22): 12481.
- Huang, Chen, Cen, et al. Heat extraction from hot dry rock by super-long gravity heat pipe: Effect of key parameters[J]. Energy, **2022**, 248: 123527.
- Chen, Huang, Cen, et al. Heat extraction from hot dry rock by super-long gravity heat pipe: Selection of working fluid [J]. Energy, **2022**, 255:124531.
- Huttrer. Geothermal power generation in the world 2015-2020 update report[C]//Proceedings world geothermal congress. 2020, 2020: 1-17.
- Zhang, Chen, Zhang. Geothermal power generation in China: Status and prospects[J]. Energy Science & Engineering, **2019**, 7(5): 1428-1450.
- Hu, Cheng, Tao. Opportunity and challenges in large-scale geothermal energy exploitation in China[J]. Critical Reviews in Environmental Science and Technology, 2021: 1-22.
- Noorollahi, Mohammadzadeh, Yousefi. Simulation of Power Production from Dry Geothermal Well Using Down-hole Heat Exchanger in Sabalan Field, Northwest Iran[J]. Natural Resources Research, **2016**, 25(2):227-239.
- Zhao, Wang, et al. Exergoeconomic analysis and optimization of a flash-binary geothermal power system[J]. Applied energy, **2016**.
- Ma, Huang, Chen, et al. Thermodynamic and economic performance of super-long gravity heat pipe geothermal power plant. 2022 [under review].
- Leveni, Manfrida, Cozzolino, et al. Energy and exergy analysis of cold and power production from the geothermal reservoir of Torre Alfina[J]. Energy, **2019**, 180:807-818.
- Ouyang, Aziz. Steady-state gas flow in pipes[J]. Journal of Petroleum Science & Engineering, **1996**, 14(3-4):137-158.
- Wang, Dai. Exergoeconomic analysis of utilizing the transcritical CO₂ cycle and the ORC for a recompression supercritical CO₂ cycle waste heat recovery: A comparative study[J]. Applied Energy, **2016**, 170:193-207.
- Turton, Bailie, Whiting, Shaeiwitz. Analysis, synthesis and design of chemical processes.3rd ed. Prentice Hall;2009.

- Yilmaz. Development and modeling of the geothermal energy based multigeneration plant for beneficial outputs: Thermo-economic and environmental analysis approach[J]. *Renewable Energy*, **2022**, 189.
- Astolfi, Romano, Bombarda, et al. Binary ORC (organic Rankine cycles) power plants for the exploitation of medium–low temperature geothermal sources-Part A: Thermodynamic optimization[J]. *Energy*, **2014**, 66(4):435-446.
- Huang, Zhang, Hu, et al. Economic analysis of heating for an enhanced geothermal system based on a simplified model in Yitong Basin, China[J]. *Energy Science and Engineering*, **2019**, 7(3).
- Lu, Zhao, Zhu, et al. Optimization and applicability of compound power cycles for enhanced geothermal systems[J]. *Applied Energy*, **2018**, 229:128-141.